Atmos. Chem. Phys. Discuss., 14, 12591–12634, 2014
www.atmos-chem-phys-discuss.net/14/12591/2014/
doi:10.5194/acpd-14-12591-2014

Atmospheric Chemistry and Physics Discussions
Open Access

Secondary Organic Aerosol (SOA) formation from hydroxyl radical oxidation and ozonolysis of monoterpenes

D. F. Zhao[1], M. Kaminski[1], P. Schlag[1], H. Fuchs[1], I.-H. Acir[1], B. Bohn[1], R. Häseler[1], A. Kiendler-Scharr[1], F. Rohrer[1], R. Tillmann[1], M. J. Wang[1], R. Wegener[1], J. Wildt[2], A. Wahner[1], and T. F. Mentel[1]

[1]Institute of Energy and Climate Research, IEK-8: Troposphere, Forschungszentrum Jülich, Jülich, 52425, Germany
[2]Institute of Bio- and Geosciences, IBG-2, Forschungszentrum Jülich, Jülich, 52425, Germany

Received: 25 April 2014 – Accepted: 6 May 2014 – Published: 16 May 2014

Correspondence to: T. F. Mentel (t.mentel@fz-juelich.de)

Published by Copernicus Publications on behalf of the European Geosciences Union.

Abstract

Oxidation by hydroxyl radical (OH) and ozonolysis are the two major pathways of daytime biogenic volatile organic compounds (VOCs) oxidation and secondary organic aerosol (SOA) formation. In this study, we investigated the particle formation of several common monoterpenes (α-pinene, β-pinene, and limonene) by OH dominated oxidation, which has seldom been investigated. OH oxidation experiments were carried out in the SAPHIR chamber in Jülich, Germany, at low NO_x (0.01–1 ppbV) and low ozone (O_3) concentration. OH concentration and OH reactivity were measured directly so that the overall reaction rates of organic compounds with OH were quantified. Multi-generation reaction process, particle growth, new particle formation, particle yield, and chemical composition were analyzed and compared with that of monoterpene ozonolysis. Multi-generation products were found to be important in OH dominated SOA formation. The relative role of functionalization and fragmentation in the reaction process of OH oxidation was analyzed by examining the particle mass and the particle size as a function of OH dose. We developed a novel method which quantitatively links particle growth to the reaction of OH with organics in a reaction system. This method was also used to analyze the evolution of functionalization and fragmentation of organics in the particle formation by OH oxidation. It shows that functionalization of organics was dominant in the beginning of the reaction (within two lifetimes of the monoterpene) and fragmentation started to be dominant after that. We compared particle formation from OH oxidation with that from pure ozonolysis. In individual experiments, growth rates of the particle size did not necessarily correlate with the reaction rate of monoterpene with OH and O_3. Comparing the size growth rates at the similar reaction rates of monoterpene with OH or O_3 indicates that generally, OH oxidation and ozonolysis had similar efficiency in particle growth. The SOA yield of α-pinene and limonene by ozonolysis was higher than that of OH oxidation. Aerosol mass spectrometry (AMS) shows SOA elemental composition from OH oxidation follows a slope shallower than -1 in the O/C vs. H/C diagram, indicating that oxidation proceeds without significant loss of

hydrogen. SOA from OH oxidation had higher H/C ratios than SOA from ozonolysis. In ozonolysis, a process with significant hydrogen loss seemed to play an important role in SOA formation.

1 Introduction

As an important class of atmospheric aerosol, organic aerosol (OA) comprises a significant fraction of aerosol mass. It accounts for around 50 % of dry tropospheric submicron aerosol mass in many urban and rural locations (Kanakidou et al., 2005; Jimenez et al., 2009; Zhang et al., 2011). OA has an important impact on air pollution, human health and climate on the regional and global scale. A large fraction of organic aerosol is contributed by secondary organic aerosol (SOA). In spite of intensive studies in the recent years, the source of SOA still has considerable uncertainties with the estimated global source ranging from 120 to 1820 $\mathrm{Tg\,a^{-1}}$ (Hallquist et al., 2009; Spracklen et al., 2011; Goldstein and Galbally, 2007). SOA is believed to mainly originate from the biogenic volatile organic compounds (BVOCs) from plants (Hallquist et al., 2009). Among them, monoterpenes are important due to their high emission rates and high reactivity (Chung and Seinfeld, 2002; Guenther et al., 1995, 2012).

The impact of SOA on the radiation budget of the Earth thus on climate depends on its particle number concentration, size distribution and composition, which affect optical properties and cloud condensation nuclei (CCN) activity of an aerosol (Andreae and Rosenfeld, 2008). Understanding particle formation and growth is therefore critical for assessing the impact of SOA.

Particle formation and growth from BVOC are mainly initiated by hydroxyl radical (OH) and ozone (O_3) oxidation during daytime. SOA formation from ozonolysis of several monoterpenes such as α-pinene, β-pinene and limonene has been studied extensively (Iinuma et al., 2005; Presto et al., 2005; Shilling et al., 2009; Yu et al., 1999; Ortega et al., 2012; Saathoff et al., 2009; Tillmann et al., 2010; Hoffmann et al., 1997; Griffin et al., 1999; Lee et al., 2006; Ma et al., 2008). However, particle formation from

OH oxidation of monoterpenes has been much less investigated and pure OH oxidation of monoterpenes has seldom been investigated due to the presence of O_3 formed in the photooxidation process (Eddingsaas et al., 2012; Ng et al., 2007; Lee et al., 2006). SOA formation from pure OH oxidation of monoterpenes regarding the reaction process such as the formation and role of multi-generation products, and the influence of OH oxidation on particle growth is not clear. Particularly, despite the importance of the OH oxidation in the particle formation, the quantitative effect of OH oxidation on particle growth is not available. Here we focus on the SOA formation from OH oxidation of monoterpenes.

It is also interesting to compare the relative importance of OH oxidation with ozonolysis of monoterpenes in particle nucleation and growth. A number of studies have investigated this question (Bonn and Moortgat, 2002; Burkholder et al., 2007; Hao et al., 2009; Mentel et al., 2009), but often at high VOC concentrations and the results are controversial. Some studies have shown the importance of ozonolysis in new particle formation (NPF) (Bonn and Moortgat, 2002) while others have emphasized the importance of OH oxidation (Burkholder et al., 2007; Hao et al., 2009; Mentel et al., 2009). Studies at the simulation chamber JPAC (Jülich Plant Aerosol Atmosphere Chamber) suggest OH and H_2SO_4 are needed to initiate NPF (Mentel et al., 2009; Kiendler-Scharr et al., 2009a, 2012; Ehn et al., 2014). Ehn et al. (2014) suggest that α-pinene ozonolysis produces a class of extreme low volatile organic compounds (ELVOC), a recently discovered highly oxidized multifunctional products, which are important for the nucleation and possibly make up 50–100 % of SOA in early stages of particle growth in Hyytiälä (Ehn et al., 2012). Regarding particle growth, Burkholder et al. (2007) stated that particle size growth rates for different oxidation sources are nearly indistinguishable. Yet, Hao et al. (2009), using the real BVOC emissions from plants, showed a much more efficient role of ozonolysis than OH oxidation in particle growth. One reason causing the different results on nucleation could be that VOC oxidation products are not the nucleating agents. Another important reason of the controversy on particle nucleation and growth is that the OH oxidation and ozonolysis have seldom been separated when comparing the SOA formation from both pathways.

In addition, the reaction rates of OH and O_3 with organics have to be quantified and comparable when one investigates the relative role of OH oxidation and ozonolysis in particle formation. To obtain the reaction rates of VOCs with OH, the OH concentration is a required parameter. However, none of these previous studies directly measured the OH concentration, which was either not stated or just modeled. Since the detailed chemistry, including HO_x generation pathways, of BVOC photooxidation is still not well understood, modeled OH concentrations may have significant uncertainties (Fuchs et al., 2013; Kaminiski, 2014; Kim et al., 2013; Whalley et al., 2011). Consequently, the relative importance of OH oxidation and ozonolysis in particle formation and growth may have large uncertainties when the comparison of both cases is based on modeled OH concentrations and corresponding reaction rates with OH.

In this study, we investigated the SOA formation and growth of several common monoterpenes, α-pinene, β-pinene and limonene, by OH oxidation at ambient relevant conditions. The OH oxidation experiments were conducted at low O_3 concentration to ensure that OH oxidation was the dominant reaction pathway. OH concentration was measured directly, as was the total reactivity (k_{OH}) of whole the reaction system with respect to OH, so that the overall reaction rates of organics with OH were directly quantified (Lou et al., 2010). Direct derivation of the overall reaction rate of organics with OH (product of OH reactivity from organics and the OH concentration) from measured parameters is a unique feature of this study. The multi-generation reaction process, particle growth, new particle formation, particle yield, and particle composition were analyzed. A novel method which quantitatively established the relationship of particle mass growth rate with the reaction rate with OH was developed for the first time here to the best of our knowledge. This method was further used to analyze the multi-generation reaction process. Particle formation by OH oxidation was compared with that by ozonolysis. Ozonolysis experiments were done in the presence of CO as OH scavenger, so that ozonolysis was the dominant reaction pathway at still ambient relevant HO_2 / RO_2 ratios. The relative roles of OH oxidation and ozonolysis in the SOA formation and particle growth were evaluated from comparisons of OH and O_3 dominated experiments. In particular, we used low VOC concentration (~ 4 ppb) with natural sunlight conditions resulting in low particle loading (sub $\mu g\,m^{-3}$ to several $\mu g\,m^{-3}$). The low particle loading allowed us to investigate the particle formation, particle growth and multi-generation reaction process under ambient relevant conditions (Presto and Donahue, 2006; Shilling et al., 2008, 2009; Pathak et al., 2007). It also minimized the condensation of early generation products with low oxidation state which is of little relevance for ambient conditions (Shilling et al., 2009; Pfaffenberger et al., 2013).

2 Experimental

2.1 Experiment setup and instrumentation

The experiments were carried out in the outdoor atmosphere simulation chamber SAPHIR (Simulation of Atmospheric PHotochemistry In a large Reaction chamber), Forschungszentrum Jülich, Germany. SAPHIR is a 270 m^3 double-wall Teflon chamber of cylindrical shape. The details of the chamber have been previously described (Rohrer et al., 2005; Bohn et al., 2005). The chamber uses natural sunlight as light source and is equipped with a louvre system to simulate dark processes when louvre is closed. It is operated with high purity synthetic air (Linde Lipur, purity 99.9999 %). A continuous flow of 7–9 $m^3\,h^{-1}$ maintains the chamber at a slight overpressure of ~ 50 Pa and compensates for the sampling losses by various instruments. This flow causes dilution of the reaction mixture with clean air at an average loss rate coefficient of $9.35 \times 10^{-6}\,s^{-1}$ (residence time of ~ 30 h), agreeing well with the dilution rates determined from measured H_2O and CO_2 time series. Pure nitrogen (Linde Lipur, purity 99.9999 %) constantly flushes the space between the inner and outer Teflon wall to prevent intrusion of contaminants into the chamber. A fan ensures mixing of trace gases within minutes, but reduces aerosol lifetime when it runs. The loss by dilution alone applies equally to suspended particles and gases. Particles in the chamber are subject to additional wall losses as reported previously (Salo et al., 2011; Fry et al., 2011). Size effects of the particle loss were neglected here because of the narrow size distribution (geometric standard deviation <1.3).

For the experiments described here, the chamber was equipped with instrumentation characterizing gas-phase and particle-phase species, as well as physical parameters including temperature, relative humidity, flow rate and photolysis frequencies.

The actinic flux and the according photolysis frequencies were provided from measurements of a spectral radiometer (Bohn et al., 2005). NO and NO_2 measurements were performed with a chemiluminescence analyzer (ECO PHYSICS TR480) equipped with a photolytic converter (ECO PHYSICS PLC760). O_3 was measured by an UV absorption spectrometer (ANSYCO model O341M). The concentrations of the VOCs were measured by a proton transfer reaction- mass spectrometer (PTR-MS, Ionicon) (Jordan et al., 2009) and gas chromatography coupled to a mass spectrometer (GC-MS, PerkinElmer) (Apel et al., 2008; Kaminiski, 2014). In the ozonolysis experiments, reactions of VOCs with O_3 in the sample line were found to cause additional monoterpene loss. Monoterpene concentrations were therefore also quantified from initial monoterpene concentrations and the losses by reaction according to the reaction rate of O_3 with monoterpenes determined from measured O_3 and by dilution.

OH, HO_2, and RO_2 radicals were measured using laser induced fluorescence (LIF). The uncertainty of the OH measurement, determined by the accuracy of the calibration of the LIF instrument, is 10 % (1σ). The details of LIF instrument were described by Fuchs et al. (2012). The OH radicals inside SAPHIR are mainly formed by the photolysis of HONO coming off the walls, and to a minor fraction by O_3 photolysis (Rohrer et al., 2005). OH reactivity (k_{OH}) was measured also using LIF and laser flash photolysis (Lou et al., 2010). The OH concentration was used to calculate the OH dose in order to better compare different experiments. The OH dose is the integral of the OH concentration over time and gives the cumulated OH concentrations to which gases and particles were exposed at a given time of an experiment. One hour exposure to typical atmospheric OH concentrations of 2×10^6 molecules cm^{-3} results in an OH dose of 7.2×10^9 molecules cm^{-3} s. The OH concentration and OH reactivity were also used to calculate the reaction rate of OH with all organics.

Particle size distributions were measured by a scanning mobility particle sizer (SMPS, TSI DMA3081/TSI CPC3785) with a size range 9.82–414.2 nm. Aerosol yield was calculated using SMPS mass concentration assuming a density of 1 g cm^{-3} to compare with previous studies in the literature. The particle mass concentration corrected for dilution and wall loss is shown here unless otherwise stated.

The chemical composition of SOA was characterized by a High-Resolution Time-of-Flight Aerosol Mass Spectrometer (HR-ToF-AMS, Aerodyne Research Inc., DeCarlo et al., 2006). Particles enter the instrument through an aerodynamic lens and are focused to a particle beam. The particles impact on a tungsten oven at 600 °C and are flash-vaporized into vapors under vacuum. The vapors are then ionized by 70 eV electron impact (EI), and the resulting ions are detected by a time-of-flight mass spectrometer operating at either a high-sensitivity mode (V-mode) or a high mass resolution mode (W-mode). In this study we used the so-called MS mode which gets the size integrated overall composition of SOA.

To characterize the degree of oxidation of particles, the O/C ratio was obtained. The O/C and H/C ratio was derived by the elemental analysis of mass spectra obtained in the high mass resolution W-mode as described by Aiken et al. (2007) and (2008). An updated procedure to calculate O/C and H/C was reported to be in development (Canagaratna et al., 2014). However, the details have not been published yet, therefore, the traditional method is still used here to derive the elemental ratio. Corrections for the minor influence of gaseous components were done before the calculation of the H/C and O/C ratio. Chamber air contains CO_2 and water vapor and both gas phase species contribute to the mass spectra. The contribution of gas phase CO_2 and water vapor to m/z 44 and to m/z 18, respectively, was inferred from measurements during periods when no particles were present. The values were subtracted to obtain

Title Page
Abstract Introduction
Conclusions References
Tables Figures
◀| |▶
◀ ▶
Back Close
Full Screen / Esc
Printer-friendly Version
Interactive Discussion

the particle signals before the elemental analysis (Allan et al., 2004). No collection efficiency correction was further used.

2.2 Experiment procedure

Two kinds of experiments, photooxidation and ozonolysis of monoterpenes were carried out under humid conditions with a starting RH ~ 75 %. The summary of the experimental conditions is shown in Table 1. All the experiments were conducted under $NO_x < \sim 1$ ppb. No NO_x was added to the chamber, and background NO_x originated mainly from the wall. In the photooxidation experiments, the O_3 concentration was <3 ppb at the start of each experiment and did not exceed 20 ppb over the course of an experiment. The OH oxidation was the dominant oxidation pathway (>~ 95 % of monoterpene loss). In a typical procedure, air in the chamber was first humidified and then the louvre system was opened for around 1.5 h. Afterwards monoterpene was injected and the reaction of monoterpene with OH occurred. After the photooxidation process, which was finished by closing the louvre system, the reaction mixtures stayed in the dark for around 1 h before they were flushed out.

The ozonolysis experiments were conducted in the dark. After humidification CO and monoterpene were added to the chamber. CO (~ 40 ppm) was used as OH scavenger to ensure that oxidation by O_3 was the dominant reaction pathway (>95 % of OH was scavenged) with little contribution of the OH oxidation to monoterpenes losses. Afterwards, O_3 generated from an UV O_3 generator was added to the chamber to start ozonolysis reaction of monoterpenes.

3 Methods

In the reaction of monoterpenes with OH and O_3, oxidation products are generated, which condense on the particle phase resulting in particle growth. In the case of OH oxidation, multi-generation products can be formed from first generation products, as

OH also reacts with saturated compounds. Particle growth depends on the condensation flux, thus the concentration of condensing products, of all generations. Since the concentration of condensing products is a function of the reaction rate, particle growth is closely related to the reaction rate of organics. We explored the relationship between particle mass growth and reaction rate of the organics with OH. When particles grow, the particle diameter enlarges and the particle mass increases due to the condensation of the reaction products. Here we use the term “particle size growth rate” to denote the particle diameter increase and “mass growth rate” to denote the particle mass increases. In the following we will establish a quantitative relationship of the particle mass growth rate with the reaction rate of OH with organics for the first time, to the best of our knowledge. Since all condensing species contribute to the particle mass growth rate, the particle mass growth rate must be related to the reaction rate of all organic species with OH, which is directly accessible from the OH concentration measurement and the k_{OH} measurement in this study. The particle mass growth rate is derived from sum of the particle mass growth due to all condensing compounds.

In a first step, we will relate the overall mass growth to the OH gas-phase reaction rates with all organic species. We describe that by a reaction of VOC i with OH, in which for simplicity one molecule of species i reacts with OH, forming one molecule of species $i+$ of the next generation:

$$i + \mathrm{OH} \longrightarrow i+ \qquad \text{(R1)}$$

According to the Raoult’s law we have the following equation, assuming the gas phase and particle phase are in equilibrium:

$$C_i^{\mathrm{g}} = \frac{C_i^{\mathrm{p}}}{C_{\mathrm{t}}^{P}} \cdot C_i^{0}, \qquad (1)$$

where C_i^{g} and C_i^{p} are the concentrations of i in the gas phase and in the particle phase (molecules cm^{-3}), C_i^{0} is the saturation vapor pressure of i expressed as gas-phase concentration of i (molecules cm^{-3}) and $C_{\mathrm{t}}^{\mathrm{p}}$ is the concentration of all molecules in the particle phase, thus $C_i^{\mathrm{p}}/C_{\mathrm{t}}^{\mathrm{p}}$ is the mole fraction of i. For high volatility species, C_i^0 is high for given C_i^{g} and thus C_i^{p} is low or even negligible. The opposite is true for low volatility species, C_i^0 is low and C_i^{p} is high.

When an infinitesimal concentration of i, $\mathrm{d}C_i^{\mathrm{g}}$, reacts via Reaction (R1), corresponding to a change of i in the particle phase, $\mathrm{d}C_i^{\mathrm{p}}$, from Eq. (1), one can get Eq. (2), because loss of i is compensated by gain in $i+$ and $C_{\mathrm{t}}^{\mathrm{p}}$ is approximately conserved

$$\mathrm{d}C_i^{\mathrm{g}} = \frac{\mathrm{d}C_i^{\mathrm{p}}}{C_{\mathrm{t}}^{P}} \cdot C_i^0. \tag{2}$$

Re-arranging Eq. (2), one can get

$$\mathrm{d}C_i^{\mathrm{p}} = \frac{C_{\mathrm{t}}^{P}}{C_i^0} \cdot \mathrm{d}C_i^{\mathrm{g}}. \tag{3}$$

Similarly, one can get

$$\mathrm{d}C_{i+1}^{\mathrm{p}} = \frac{C_{\mathrm{t}}^{P}}{C_{i+1}^0} \cdot \mathrm{d}C_{i+1}^{\mathrm{g}}. \tag{4}$$

For the change of the particle mass concentration (m, µg m^{-3}) due to the reaction of species i by Reaction (R1), we have

$$\left(\frac{\mathrm{d}m}{\mathrm{d}t}\right)_i = \frac{\mathrm{d}m_{i+}^{\mathrm{p}}}{\mathrm{d}t} + \frac{\mathrm{d}m_i^{\mathrm{p}}}{\mathrm{d}t}. \tag{5}$$

Title Page
Abstract | Introduction
Conclusions | References
Tables | Figures
◀| |▶
◀ ▶
Back | Close
Full Screen / Esc
Printer-friendly Version
Interactive Discussion

$\mathrm{d}m_i^\mathrm{p}$ ($\mu\mathrm{g\,m^{-3}}$) and $\mathrm{d}C_i^\mathrm{p}$ can be related by

$$\mathrm{d}m_i^\mathrm{p} = \frac{\mathrm{d}C_i^\mathrm{p} \cdot M_i 10^6 \cdot 10^6}{N_\mathrm{A}}, \tag{6}$$

where M_i is the molecular weight of species i ($\mathrm{mol\,kg^{-1}}$) and N_A is Avogadro's Constant.

Similarly with Eq. (6), for species $i+$, one can get

$$\mathrm{d}m_{i+}^\mathrm{p} = \frac{\mathrm{d}C_{i+}^\mathrm{p} \cdot M_{i+} 10^6 \cdot 10^6}{N_\mathrm{A}}. \tag{7}$$

By applying the relationship of i and $i+$ in the Reaction (R1), we express,

$$\mathrm{d}C_{i+}^\mathrm{g} = -\mathrm{d}C_i^\mathrm{g}. \tag{8}$$

Substituting Eqs. (3), (4), (6–8) into Eq. (5), one can get

$$\left(\frac{\mathrm{d}m}{\mathrm{d}t}\right)_i = \frac{\mathrm{d}C_i^\mathrm{g}}{\mathrm{d}t} \cdot C_\mathrm{t}^\mathrm{p} \frac{10^6 \cdot 10^6}{N_\mathrm{A}} \left(\frac{M_i}{C_i^0} - \frac{M_{i+}}{C_{i+}^0}\right). \tag{9}$$

Assuming M_{i+} and M_i are similar, with an average molecular weight M, one can get

$$m_\mathrm{t} = C_\mathrm{t}^\mathrm{p} \frac{10^6 \cdot 10^6}{N_\mathrm{A}} M, \tag{10}$$

where m_t is total particle mass concentration.

Substituting Eq. (10) into Eq. (9), one can get

$$\left(\frac{\mathrm{d}m}{\mathrm{d}t}\right)_i = \frac{\mathrm{d}C_i^\mathrm{g}}{\mathrm{d}t} \cdot m_\mathrm{t} \left(\frac{1}{C_i^0} - \frac{1}{C_{i+}^0}\right). \tag{11}$$

If we relax our assumption that one molecule of $i+$ is formed from the loss of one molecule of i in the Reaction (R1), e.g. in case of fragmentation, Eq. (11) still holds (as shown in Appendix A).

According to the reaction of i with OH, we have

$$\frac{\mathrm{d}C_i^{\mathrm{g}}}{\mathrm{d}t} = -R_{\mathrm{OH},i}, \tag{12}$$

where $R_{\mathrm{OH},i}$ is the reaction rate of species i with OH.

Substitute Eq. (12) into Eq. (11),

$$\left(\frac{\mathrm{d}m}{\mathrm{d}t}\right)_i = R_{\mathrm{OH},i} \cdot m_\mathrm{t} \left(\frac{1}{C_{i+}^0} - \frac{1}{C_i^0}\right). \tag{13}$$

Considering all the species contributing to the particle phase, we have

$$\frac{\mathrm{d}m_\mathrm{t}}{\mathrm{d}t} = \sum_i R_{\mathrm{OH},i} m_\mathrm{t} \left(\frac{1}{C_{i+}^0} - \frac{1}{C_i^0}\right). \tag{14}$$

Re-arrange Eq. (14),

$$\frac{\mathrm{d}m_\mathrm{t}}{\mathrm{d}t} = m_\mathrm{t} \sum_i R_{\mathrm{OH},i} \frac{\sum\limits_{i=1} R_{\mathrm{OH},i} \left(\frac{1}{C_{i+}^0} - \frac{1}{C_i^0}\right)}{\sum\limits_i R_{\mathrm{OH},i}}. \tag{15}$$

Summing up all the species, we have

$$R_\mathrm{OH} = \sum_i R_{\mathrm{OH},i}, \tag{16}$$

wherein R_OH is the reaction rate of all organics with OH.

In the next step, we will derive a system characterizing quantity in order to overcome the underdetermined knowledge about the individual components due to the complexity of monoterpene degradation. We define a new metric, $\mathrm{GE}_{\mathrm{OH}}(t,i)$ (particle growth efficiency in respect to the reaction of OH with all organics in the whole reaction system (including the VOCs and their oxidation products)) in Eq. (17) for species i:

$$\mathrm{GE}_{\mathrm{OH}}(t,i) = \frac{1}{C^0_{i+}} - \frac{1}{C^0_i}. \tag{17}$$

One can also define

$$\frac{\sum_i R_{\mathrm{OH},i} \cdot \frac{1}{C^0_{i+}}}{\sum_i R_{\mathrm{OH},i}} = \frac{1}{\overline{C}^0_{i+}}, \tag{18}$$

and

$$\frac{\sum_i R_{\mathrm{OH},i} \cdot \frac{1}{C^0_{i}}}{\sum_i R_{\mathrm{OH},i}} = \frac{1}{\overline{C}^0_{i}}. \tag{19}$$

$\overline{C}^0_{i+}$ and $\overline{C}^0_i$ are obtained from the average of $1/C^0_i$ for all organics weighed by the reaction rate with OH, which in a certain way reflect the overall saturation vapor pressures. Substituting Eqs. (16), (18) and (19) into Eq. (15), one can get

$$\frac{\mathrm{d}m_\mathrm{t}}{\mathrm{d}t} = R_{\mathrm{OH}} \cdot m_\mathrm{t} \cdot \left(\frac{1}{\overline{C}^0_{i+}} - \frac{1}{\overline{C}^0_i} \right). \tag{20}$$

Then, as Eq. (17), one can also define

$$\mathrm{GE}_{\mathrm{OH}}(t) = \frac{1}{\overline{C}^0_{i+}} - \frac{1}{\overline{C}^0_i}. \tag{21}$$

$\mathrm{GE_{OH}}(t)$, a system describing quantity, is derived here in order to characterize the chemical system. It is an overall average of $\mathrm{GE_{OH}}(t,i)$ weighted by reaction rate with OH of each species. Substituting Eq. (21) into Eq. (20),

$$\frac{\mathrm{d}m_\mathrm{t}}{\mathrm{d}t} = R_\mathrm{OH} \cdot m_\mathrm{t} \cdot \mathrm{GE_{OH}}(t) \tag{22}$$

Arranging Eq. (22), one can get

$$\mathrm{GE_{OH}}(t) = \frac{\frac{\mathrm{d}m_\mathrm{t}}{\mathrm{d}t}}{R_\mathrm{OH} \cdot m_\mathrm{t}} \tag{23}$$

Equation (22) shows a quantitative relationship of the particle mass growth rate with the reaction rate of OH of all organics, which are linked by $\mathrm{GE_{OH}}(t)$. $\mathrm{GE_{OH}}(t)$ is the mass growth rate normalized to the OH reaction rate and mass concentration, i.e. the mass growth rate per OH reacted per aerosol mass concentration (as shown in Eq. 23). It is a metric of how effectively the reaction with OH changes the mass growth rate at a given mass concentration in a reaction system. $\mathrm{GE_{OH}}(t)$ has a unit of $\mathrm{cm^3\,molecules^{-1}}$ (reciprocal of the unit of the concentration). It relates to the change of overall saturated concentration of reaction products upon reaction with OH as shown in Eq. (21). In our case, where we measured OH and k_OH, R_OH is directly accessible. The reaction rate of OH with all organics was calculated using the measured k_OH and subtracting the OH reactivity of inorganic species (NO, $\mathrm{NO_2}$, CO).

4 Results and discussion

4.1 Multi-generation reaction process and particle growth

Figure 1 shows the time dependent particle "growth curve" (particle mass concentration as a function of monoterpene consumed) from the OH oxidation of α-pinene, β-pinene and limonene. After one monoterpene life time (when the monoterpene concentration decreased to 1/e of the initial concentration), only 13 %, 33 %, and 25 % of the total mass was reached for the OH oxidation of α-pinene, β-pinene and limonene, respectively. This indicates the importance of higher generation products in the SOA formation from OH oxidation of each monoterpene (Ng et al., 2006). Our results differ from several previous studies carried out at much higher VOC and SOA concentrations (Ng et al., 2006, 2007). Ng et al. (2006) showed that the time dependent growth curve is almost linear for terpenes with one double bond such as α-pinene and β-pinene. The difference can be attributed to the difference of VOC and the particle concentration. At high particle mass loading, the species with relatively high volatility such as first generation products significantly condense. At low particle loading, only the species with relatively low volatility which require more oxidation steps (by OH) can significantly condense onto the particle phase. Consequently, the later generation products play important roles in the particle formation in this study. The importance of multi-generation products agrees with Eddingsaas et al. (2012), who showed that particle growth continues well after two lifetimes of α-pinene with respect to OH oxidation at low NO_x condition.

In contrast to OH oxidation, the total mass concentration increased roughly linearly with the consumed monoterpene concentration for the ozonolysis of each monoterpene (Fig. A1). The time-dependent growth curves of three monopterpenes in the ozonolysis experiments agree with previous studies (Ng et al., 2006; Zhang et al., 2006) and a recent study of Ehn et al. (2014) showing the formation of first generation products as the rate-limiting step. There was an apparent positive offset on the hydrocarbon consumed for α-pinene and β-pinene, and barely an offset for limonene, since the reaction products needed to reach their saturation concentration to condense on the particle phase. For limonene, within the time resolution of our measurement they reached the saturation concentration immediately. The offsets are consistent with the findings of the nucleation threshold of monoterpenes (Bernard et al., 2012; Mentel et al., 2009). The differences of the threshold concentrations of different monoterpenes are related to their properties.

To further investigate the role of multi-generation oxidation by OH, the particle mass concentration and the median size as a function of OH dose are shown in Fig. 2. For all three monoterpenes, the particle mass concentration increased and size grew as the reaction proceeded and monoterpene reacted with OH (increasing OH dose). Then the increase of the mass concentration and growth of size with respect to OH dose started to slow down gradually and subsequently leveled off. Particle size even decreased after leveling off in the case of limonene. For α-pinene, the photooxidation reaction stopped in the dark after the louvre system of the chamber had been closed before the particle mass could level off.

In the beginning of the reaction, monoterpene reacted with OH generating low volatility compounds by the functionalization process, which condensed on the particle and resulted in the particle mass increase and size growth. These condensing compounds still continued reacting with OH which could lead to functionalization as well as fragmentation. Fragmentation can generate high volatility species thus promote evaporation. Since fragmentation increased with O/C and the role of functionalization decreased (Kroll et al., 2009; Chacon-Madrid and Donahue, 2011; Chacon-Madrid et al., 2010), the role of fragmentation became more and more significant as the reaction proceeded. When the fragmentation dominated over functionalization, the overall volatility of the products increased, i.e., the saturated vapor pressures decreased. When the overall concentration of condensing species dropped below the overall saturation concentration due to the reaction and dilution, a net negative flux of condensable compounds occurred and these compounds started to evaporate from the particles. Therefore, the particle size first reached a plateau and even diminished as observed in the limonene oxidation experiment.

Moreover, time series of $\mathrm{GE_{OH}}(t)$, the metric of particle growth efficiency due to reaction with OH, shed light on the role of functionalization and fragmentation in the reaction process. Figure 3 shows that the $\mathrm{GE_{OH}}(t)$ time series and the particle mass concentration as well as total OH reactivity of organics for comparison. $\mathrm{GE_{OH}}(t)$ increased fast at the beginning of the reaction and then gradually decreased. The change of $\mathrm{GE_{OH}}(t)$

reflects the evolution of the overall volatility of organics undergoing reaction with OH and the relative role of functionalization and fragmentation.

In the beginning, functionalization played a dominant role. The reaction product had a lower volatility than the reactant, i.e., lower saturated concentration, therefore $GE_{OH}(t)$ is positive (refer to Eq. 21). As the volatility became lower, $GE_{OH}(t)$ increased. In the subsequent reaction, as the products got more oxidized and O/C ratio of products increased, the fragmentation of the compounds became more and more significant. The fragmentation cleaved the carbon frame and formed some smaller molecules with higher volatility. This caused the increase of overall volatility of the organics to slow down until it stopped and volatility even increased after the reaction with OH, that is, $GE_{OH}(t)$ decreased. When the overall volatility of the reactants is equal to that of the products, $GE_{OH}(t)$ is equal to zero. $GE_{OH}(t)$ was observed to decrease to almost zero or even negative (Fig. 3c). From Fig. 3 one can recognize that the fragmentation started to play an important role in the relatively early period of the reaction (within approximate two lifetimes) when the mass concentration was still low. For comparison, the H/C and O/C time series of SOA are also shown in Fig. 3. The change of H/C and O/C ratio supports our analysis of the role of functionalization and fragmentation. $GE_{OH}(t)$ decreased dramatically at the same time when O/C ratio increased to around 0.4 and leveled off. Accordingly, H/C started to decrease from the beginning of the reaction and then leveled off at the same time as O/C. For reference, Kroll et al. (2009) showed that for the reaction of squalane with OH fragmentation dominates when the organics are moderately oxidized ($O/C \approx 0.4$). The branching ratio of fragmentation and functionalization has been parameterized as the power law of O/C (Donahue et al., 2012; Jimenez et al., 2009). Based on the $GE_{OH}(t)$ time series, the particle formation efficiency in respect to the reaction with OH was high in the beginning of the reaction although the mass growth rate was low. In contrast, at the later period of the reaction, the efficiency of OH reaction to formation of particle was low and the mass growth was mainly attributed to the role of favorable partitioning at higher organics mass loading.

In addition, $\mathrm{GE}_{\mathrm{OH}}(t)$ can shed some light on the vapor pressure of the reaction products. Since the volatility of products decreases around one to two order of magnitude in functionalization (Ziemann and Atkinson, 2012), in the beginning of the reaction when functionalization dominated, $C^0_{n,i+} \ll C^0_{n,i}$. Then, based on Eq. (21), the following equation is tenable:

$$\mathrm{GE}_{\mathrm{OH}}(t) = \frac{1}{\overline{C}^{0}_{n,i+}} \tag{24}$$

Since $\overline{C}^{0}_{i+}$ is an average saturation pressure weighed in a certain way as shown in Eq. (18). Equation (24) provides a rough estimate of the overall vapor pressure of the organics from experimentally obtained $\mathrm{GE}_{\mathrm{OH}}(t)$. In the case of β-pinene OH oxidation, the overall vapor pressure varied from around 6×10^{-5} to 1×10^{-3} Pa. As a reference, the lower value is of the same order of magnitude as the estimated vapor pressure of norpinonic acid based on the structure-activity relationship (Compernolle et al., 2011).

We established the relationship of particle mass growth rate with the reaction rate of OH with organics. The relationship of the particle size growth rate with the reaction rate is not straightforward. The size growth rate is proportional to the deviation of the concentrations of condensing species from their equilibrium concentrations, while the reaction rate of monoterpene with OH and O_3 is proportional to the rate of the increase of condensing species concentrations, i.e., the derivative of the concentrations. Additionally, the equilibrium concentrations of the each species changes continuously with their varying molar fractions in the particle phase during the reaction. Therefore, the reaction rate is only indirectly related to the size growth rate and should not necessarily correlate with size growth rate as observed in Fig. 4a and c. Still some variations in the size growth rate and mass growth rate follow the variations of the reaction rate of OH with organics and/or reaction rate of OH with monoterpenes (such as Fig. 4a–c). These variations in the reaction rates were mostly caused by sudden changes of the OH concentration due to variations of solar radiation affected by clouds.

Comparing the particle growth of OH oxidation and ozonolysis, the ratios of the peak OH reaction rate to the O_3 reaction rate for α-pinene, β-pinene and limonene were around 1.0, 1.2 and 0.5, respectively. The corresponding ratios of peak size growth rates for OH oxidation to that for ozonolysis were around 1.0, 1.5 and 1.1. At the similar monoterpene concentration and similar reaction rate of OH or O_3 with monoterpene, the size growth rates were comparable. This comparison indicates that generally OH oxidation and ozonolysis have similar efficiency in the particle growth of α-pinene, β-pinene and limonene. This result is in contrast with the study of Hao et al. (2009), who found a much more efficient role of ozonolysis in particle growth from plant emissons than that of OH oxidation. Yet, our study agrees with Burkholder et al. (2007), reporting the nearly indistinguishable particle size growth rate for different oxidation sources. Nevertheless, our experiments differ from both of these studies in terms of OH scavenger used (CO used in this study, cyclohexane and butanol in Burkholder et al., 2007; Hao et al., 2009, respectively). Since CO can cause a higher HO_2/RO_2 ratio than cyclohexane and butanol, different OH scavengers could result in different radical chemistry which could further alter the reaction pathways and products and finally could affect particle growth.

4.2 New particle formation and SOA yield

Figure 5 shows the particle number concentration, mass concentration, surface concentration and median diameter of aerosol from each monoterpene by OH oxidation and ozonolysis. The particle number concentrations of OH oxidation experiments were around 2000–6000 $\# cm^{-3}$. The particle number concentrations from the ozonolysis of monoterpene were around 0.4×10^5–1.6×10^5 $\# cm^{-3}$, which were much higher than that generated by OH oxidation of the respective monoterpene. However, we have no indications what compounds eventually initiated the new particle formation (NPF) from ozonolysis in the SAPHIR chamber made of Teflon-FEP. The role of OH oxidation and ozonolysis in the SOA nucleation and growth from monoterpenes have been reported by a number of studies before with inclusive results (Bonn and Moortgat, 2002;

Burkholder et al., 2007; Hao et al., 2009; Mentel et al., 2009), however experiments were performed often at higher VOC and aerosol concentrations. In addition, the role of monoterpene ozonolysis in nucleation in the presence of SO_2 (without OH scavenger) was shown by Ortega et al. (2012). In our JPAC glass chamber (Mentel et al., 2009), OH and H_2SO_4 are needed to initiate NPF (Mentel et al., 2009; Kiendler-Scharr et al., 2009a, 2012; Ehn et al., 2014); it is possible that in Teflon chambers in absence of OH and significant H_2SO_4 formation, other unknown compounds (perfluorinated acids) may play a role.

SOA yields observed in this study are similar to those observed before. SOA yield of α-pinene, β-pinene, and limonene by OH oxidation was 2.5 %, 6.8 % and 16.9 % at the aerosol loading of 0.5, 0.8 and 2.1 $\mu g\,m^{-3}$, respectively (Fig. A2). Since the multi-generation oxidation was the rate-limiting step, the "dynamic" yield from OH oxidation was not used (Presto and Donahue, 2006; Ng et al., 2006) and only final yield was derived. The aerosol yield of α-pinene OH oxidation is roughly consistent with a study (Henry et al., 2012), although there were only few data points in that study overlapping the range of our study (<1 $\mu g\,m^{-3}$, exact data not available from Henry et al., 2012, thus not shown in the figure). For β-pinene and limonene, there are few data of the aerosol yield of OH oxidation available especially at the aerosol loading similarly low to this study in the literature (Griffin et al., 1999; Hoffmann et al., 1997; Kim et al., 2012).

The particle yields for the ozonolysis experiments for α-pinene, β-pinene and limonene (shown in Fig. A2, together with selected literature data at similar mass loadings) are approximately in the range of or slightly higher than literature values (Pathak et al., 2007, 2008; Shilling et al., 2009; Saathoff et al., 2009; Zhang et al., 2006). The difference can be attributed to the difference in experimental conditions such as OH scavenger type, the temperature and RH etc. The aerosol yields of ozonolysis for α-pinene and limonene were higher than that of OH oxidation, while similar between both oxidation cases for β-pinene. The difference in the aerosol yield could be due to the difference in reaction pathways and products composition between the OH oxidation and ozonolysis. Also the temperature of the ozonolysis was lower than the OH oxidation, which may affect the SOA yield. However, Pathak et al. (2007) only observed weak dependence of SOA yield from α-pinene ozonolysis on temperature from 288 to 303 K, and especially for at low α-pinene reacted there is little temperature dependence. Therefore, temperature is likely to have only minor effect on the SOA yield of ozonolysis here.

4.3 Chemical composition

The H/C ratio vs. the O/C ratio plot known as Van Krevelen diagram for the aerosol from OH oxidation and ozonolysis is shown in Fig. 6. The O/C ranges for both oxidation cases were similar, around 0.3–0.6. The O/C ranges are consistent with the O/C range from α-pinene photooxidaton and ozonolysis (Chhabra et al., 2011; Ng et al., 2011; Pfaffenberger et al., 2013). They also agree with the O/C value (0.33–0.68) in a plant chamber observations for monoterpene-dominated emission mixtures (Kiendler-Scharr et al., 2009b) when one calculates O/C from f44 (the ratio of signal at m/z 44 (CO_2^+) to total organics) (Ng et al., 2010).

The H/C ratio of SOA from OH oxidation was around 1.4–1.6, slightly lower than that of the precursor monoterpene (H/C = 1.6). This indicates that during the reaction oxygen was added to the monoterpene without significant loss of hydrogen especially in the initial period of the reaction. SOA from OH oxidation of all three monoterpenes tended to follow a slope of shallower than −1 starting from monoterpene in the Van Krevelen diagram (Fig. 6a–c). This is in contrast to the findings by Heald et al. (2010), but consistent with those of Chhabra et al. (2011) and Ng et al. (2011). Heald et al. (2010) found atmospheric OA follows a slope of −1 in the Van Krevelen diagram based on a variety of ambient and laboratory studies, which indicates the addition of carboxylic group or equal addition of carbonyl and hydroxyl group to average saturated hydrocarbon. However, in this study, monoterpenes are unsaturated hydrocarbons. Therefore, oxidation such as adding two carbonyl or carboxylic acid groups per double bond can happen without significant loss of hydrogen, resulting in a slope shallower than −1. This finding agrees with Chhabra et al. (2011) who investigated a series of unsaturated hydrocarbons. Oxidation without significant loss of hydrogen can be also achieved by a "non-classsical" path, inserting O (O–O) into C–H (C–C) bonds (Ehn et al., 2012, 2014). In the classical path, increasing carbonylization/carboxylization in saturated parts of the condensable molecules leads to increase of O/C at simultaneous decrease of H/C. After the initial period of particle formation (around one lifetime of monoterpene), elemental composition of SOA from OH oxidation seemed to follow a slope of more close to −1. This indicates that the condensable species forming SOA underwent more efficient hydrogen loss upon oxidation. Since the double bond is more reactive and reacted first, the carbon chain in the initial products became more saturated. Further "classical" oxidation of these products required hydrogen loss as ambient organic aerosols (Heald et al., 2010). For the SOA from OH oxidation, H/C decreased and O/C increased generally during the reaction. For β-pinene, O/C even decreased again at the later period of the reaction (Fig. 6b). This could be due to oligomerisation after condensation forming larger units while releasing of water (formation of esters) or O_2 (dimerization of hydroperoxides) or be due to fragmentation of the products leading to more volatile products.

For SOA from ozonolysis, the H/C was around 1.2–1.4, which was distinctively lower than that of the OH oxidation. The lower H/C in the ozonolysis compared to photooxidation was reported by Chhabra et al. (2011). It seemed that a process with significant hydrogen loss such as addition of carbonyl plays a more important role in the SOA formation from ozonolysis compared to OH oxidation.

In the individual ozonolysis experiments, the O/C and H/C reached a stable value shortly (<1 h) after the reaction started and then did not show significant change. The different trend with time between the OH oxidation and ozonolysis was caused by the different reaction process. In the OH oxidation, after the particle formed, the reaction products were subject to further reaction with OH. Hence the reaction products, H/C and O/C kept evolving. In contrast, in the ozonolysis the reaction ceased once O_3 reacted with monoterpene. Therefore, there was no further significant change in the O/C and H/C in the ozonolysis.

5 Conclusions

In this study, the SOA formation from OH oxidation of several monoterpenes, α-pinene, β-pinene and limonene was investigated at ambient relevant conditions (low OA concentration, low VOC and NO_x concentrations) and was compared with the SOA formation from ozonolysis (CO as the OH scavenger). The OH dominant oxidation was achieved at low O_3 concentration. Multi-generation reaction process, particle growth, new particle formation, particle yield, and chemical composition were analyzed.

The aerosol "growth curve" reflected the importance of multi-generation products in the OH oxidation of three monoterpenes. In the OH oxidation, we found the transition of functionalization and fragmentation through the analysis of the evolution of particle size and particle mass as a function of OH dose. A novel method was developed which quantitatively linked the particle mass growth rate to the reaction rate of OH with organics via a metric of particle growth efficiency of OH reaction. This method was also used to examine the role of functionalization and fragmentation during the particle formation of monoterpenes by OH oxidation. Functionalization was found dominant in the beginning of the reaction (within approximately two lifetimes of the monoterpene) and fragmentation started to be dominant after that. The particle growth efficiency of the OH reaction was high in the beginning of the experiment, although the mass growth rate was low due to the low particle mass. This new method also provided an estimation of overall vapor pressure of the products when functionalization was dominant. We show that the overall vapor pressures vary from 10^{-5} to 10^{-3} Pa in the OH oxidation. The method of quantitatively linking particle mass growth rate to the OH reaction rate with organics will be used in other VOC systems and ambient measurements to further investigate the influence of OH oxidation on the particle growth.

The particle size growth rate did not necessarily correlate directly with the reaction rate of monoterpenes with OH and O_3 in individual experiments. Particle size growth rates induced by the reaction with OH and ozonolysis were comparable in this study at similar reaction rates of the monoterpenes with OH and O_3. This indicates that OH oxidation and ozonolysis have comparable efficiency in particle growth. The SOA yields of OH oxidation and ozonolysis in this study are generally consistent with the values in the literature. Ozonolysis of α-pinene and limonene produced a higher aerosol yield than the respective OH oxidation.

SOA from monoterpene OH oxidation generally followed a slope of shallower than -1 in the Van Krevelen diagrams, indicative of a process without significant loss of hydrogen during the oxidation. In the later period of the reaction (after around one lifetime of monoterpene), SOA followed a slope of close to -1. SOA from OH oxidation had a higher H/C than that from ozonolysis. In ozonolysis, a process with significant hydrogen loss such as addition of carbonyl seemed to play an important role in SOA formation.

Appendix A

Additional equations for the relationship of particle mass growth and the reaction rate with OH

In the case of fragmentation, there could be more than one product, $i+\_1, i+\_2, i+\_p$. Equation (11) in the main text is in a slightly different form.

$$\left(\frac{\mathrm{d}m}{\mathrm{d}t}\right)_i = \frac{\mathrm{d}C_i^{\mathrm{g}}}{\mathrm{d}t} \cdot m_{\mathrm{t}} \left(\sum_{k=1}^{\mathrm{p}} \frac{1}{C^0_{i+\_k}} - \frac{1}{C^0_i} \right) \tag{A1}$$

One can define

$$\frac{1}{C^0_{\mathrm{avg},i+}} = \sum_{k=1}^{\mathrm{p}} \frac{1}{C^0_{i+\_k}} \tag{A2}$$

Fragmentation usually generates one small volatile molecule and one less volatile molecule (assuming species P_{i+_1}).

$$\frac{1}{C^0_{\mathrm{avg},i+}} \approx \frac{1}{C^0_{i+\_1}} \tag{A3}$$

Thus $i+\_1$ can directly correspond to $i+$ in Eq. (11) in the main text and will not change the format of Eq. (11).

Acknowledgements. M. J. Wang would like to thank China Scholarship Council for funding the joint PhD program.

The service charges for this open access publication
have been covered by a Research Centre of the
Helmholtz Association.

References

Aiken, A. C., DeCarlo, P. F., and Jimenez, J. L.: Elemental analysis of organic species with electron ionization high-resolution mass spectrometry, Anal. Chem., 79, 8350–8358, doi:10.1021/ac071150w, 2007.

Aiken, A. C., Decarlo, P. F., Kroll, J. H., Worsnop, D. R., Huffman, J. A., Docherty, K. S., Ulbrich, I. M., Mohr, C., Kimmel, J. R., Sueper, D., Sun, Y., Zhang, Q., Trimborn, A., Northway, M., Ziemann, P. J., Canagaratna, M. R., Onasch, T. B., Alfarra, M. R., Prevot, A. S. H., Dommen, J., Duplissy, J., Metzger, A., Baltensperger, U., and Jimenez, J. L.: O/C and OM/OC ratios of primary, secondary, and ambient organic aerosols with high-resolution time-of-flight aerosol mass spectrometry, Environ. Sci. Technol., 42, 4478–4485, doi:10.1021/es703009q, 2008.

Allan, J. D., Delia, A. E., Coe, H., Bower, K. N., Alfarra, M. R., Jimenez, J. L., Middlebrook, A. M., Drewnick, F., Onasch, T. B., Canagaratna, M. R., Jayne, J. T., and Worsnop, D. R.: A generalised method for the extraction of chemically resolved mass spectra from aerodyne aerosol mass spectrometer data, J. Aerosol Sci., 35, 909–922, doi:10.1016/j.jaerosci.2004.02.007, 2004.

Andreae, M. O. and Rosenfeld, D.: Aerosol-cloud-precipitation interactions. Part 1. The nature and sources of cloud-active aerosols, Earth Sci. Rev., 89, 13–41, doi:10.1016/j.earscirev.2008.03.001, 2008.

Apel, E. C., Brauers, T., Koppmann, R., Bandowe, B., Bossmeyer, J., Holzke, C., Tillmann, R., Wahner, A., Wegener, R., Brunner, A., Jocher, M., Ruuskanen, T., Spirig, C., Steigner, D., Steinbrecher, R., Alvarez, E. G., Muller, K., Burrows, J. P., Schade, G., Solomon, S. J., Ladstatter-Weissenmayer, A., Simmonds, P., Young, D., Hopkins, J. R., Lewis, A. C., Legreid, G., Reimann, S., Hansel, A., Wisthaler, A., Blake, R. S., Ellis, A. M., Monks, P. S., and Wyche, K. P.: Intercomparison of oxygenated volatile organic compound measurements at the SAPHIR atmosphere simulation chamber, J. Geophys. Res.-Atmos., 113, D20307, doi:10.1029/2008jd009865, 2008.

Atkinson, R. and Arey, J.: Atmospheric degradation of volatile organic compounds, Chem. Rev., 103, 4605–4638, doi:10.1021/cr0206420, 2003.

Bernard, F., Fedioun, I., Peyroux, F., Quilgars, A., Daele, V., and Mellouki, A.: Thresholds of secondary organic aerosol formation by ozonolysis of monoterpenes measured in a laminar flow aerosol reactor, J. Aerosol Sci., 43, 14–30, doi:10.1016/j.jaerosci.2011.08.005, 2012.

Bohn, B., Rohrer, F., Brauers, T., and Wahner, A.: Actinometric measurements of NO_2 photolysis frequencies in the atmosphere simulation chamber SAPHIR, Atmos. Chem. Phys., 5, 493–503, doi:10.5194/acp-5-493-2005, 2005.

Bonn, B. and Moorgat, G. K.: New particle formation during α- and β-pinene oxidation by O_3, OH and NO_3, and the influence of water vapour: particle size distribution studies, Atmos. Chem. Phys., 2, 183–196, doi:10.5194/acp-2-183-2002, 2002.

Burkholder, J. B., Baynard, T., Ravishankara, A. R., and Lovejoy, E. R.: Particle nucleation following the O_3 and OH initiated oxidation of alpha-pinene and beta-pinene between 278 and 320 K, J. Geophys. Res.-Atmos., 112, D10216, doi:10.1029/2006jd007783, 2007.

Canagaratna, M., Massoli, P., Jimenez, J. L., Kessler, S. H., Chen, Q., Hildebrandt, L., Fortner, E., Williams, L. R., Wilson, K. R., Surratt, J. D., Donahue, N. M., Kroll, J., Jayne, J. T., and Worsnop, D. R.: Improved calibration of O/C and H/C Ratios obtained by Aerosol Mass Spectrometry of organic species, in preparation, 2014.

Chacon-Madrid, H. J. and Donahue, N. M.: Fragmentation vs. functionalization: chemical aging and organic aerosol formation, Atmos. Chem. Phys., 11, 10553–10563, doi:10.5194/acp-11-10553-2011, 2011.

Chacon-Madrid, H. J., Presto, A. A., and Donahue, N. M.: Functionalization vs. fragmentation: *n*-aldehyde oxidation mechanisms and secondary organic aerosol formation, Phys. Chem. Chem. Phys., 12, 13975–13982, doi:10.1039/c0cp00200c, 2010.

Chhabra, P. S., Ng, N. L., Canagaratna, M. R., Corrigan, A. L., Russell, L. M., Worsnop, D. R., Flagan, R. C., and Seinfeld, J. H.: Elemental composition and oxidation of chamber organic aerosol, Atmos. Chem. Phys., 11, 8827–8845, doi:10.5194/acp-11-8827-2011, 2011.

Chung, S. H. and Seinfeld, J. H.: Global distribution and climate forcing of carbonaceous aerosols, J. Geophys. Res.-Atmos., 107, 4407, doi:10.1029/2001jd001397, 2002.

Compernolle, S., Ceulemans, K., and Müller, J.-F.: EVAPORATION: a new vapour pressure estimation methodfor organic molecules including non-additivity and intramolecular interactions, Atmos. Chem. Phys., 11, 9431–9450, doi:10.5194/acp-11-9431-2011, 2011.

DeCarlo, P. F., Kimmel, J. R., Trimborn, A., Northway, M. J., Jayne, J. T., Aiken, A. C., Gonin, M., Fuhrer, K., Horvath, T., Docherty, K. S., Worsnop, D. R., and Jimenez, J. L.: Field-deployable, high-resolution, time-of-flight aerosol mass spectrometer, Anal. Chem., 78, 8281–8289, doi:10.1021/ac061249n, 2006.

Donahue, N. M., Henry, K. M., Mentel, T. F., Kiendler-Scharr, A., Spindler, C., Bohn, B., Brauers, T., Dorn, H. P., Fuchs, H., Tillmann, R., Wahner, A., Saathoff, H., Naumann, K. H., Mohler, O., Leisner, T., Muller, L., Reinnig, M. C., Hoffmann, T., Salo, K., Hallquist, M., Frosch, M., Bilde, M., Tritscher, T., Barmet, P., Praplan, A. P., DeCarlo, P. F., Dommen, J., Prevot, A. S. H., and Baltensperger, U.: Aging of biogenic secondary organic aerosol via gas-phase OH radical reactions, P. Natl. Acad. Sci. USA, 109, 13503–13508, doi:10.1073/pnas.1115186109, 2012.

Eddingsaas, N. C., Loza, C. L., Yee, L. D., Chan, M., Schilling, K. A., Chhabra, P. S., Seinfeld, J. H., and Wennberg, P. O.: α-pinene photooxidation under controlled chemical conditions – Part 2: SOA yield and composition in low- and high-NO_x environments, Atmos. Chem. Phys., 12, 7413–7427, doi:10.5194/acp-12-7413-2012, 2012.

Ehn, M., Kleist, E., Junninen, H., Petäjä, T., Lönn, G., Schobesberger, S., Dal Maso, M., Trimborn, A., Kulmala, M., Worsnop, D. R., Wahner, A., Wildt, J., and Mentel, Th. F.: Gas phase formation of extremely oxidized pinene reaction products in chamber and ambient air, Atmos. Chem. Phys., 12, 5113–5127, doi:10.5194/acp-12-5113-2012, 2012.

Ehn, M., Thornton, J. A., Kleist, E., Sipila, M., Junninen, H., Pullinen, I., Springer, M., Rubach, F., Tillmann, R., Lee, B., Lopez-Hilfiker, F., Andres, S., Acir, I.-H., Rissanen, M., Jokinen, T., Schobesberger, S., Kangasluoma, J., Kontkanen, J., Nieminen, T., Kurten, T., Nielsen, L. B., Jorgensen, S., Kjaergaard, H. G., Canagaratna, M., Maso, M. D., Berndt, T., Petaja, T., Wahner, A., Kerminen, V.-M., Kulmala, M., Worsnop, D. R., Wildt, J., and Mentel, T. F.: A large source of low-volatility secondary organic aerosol, Nature, 506, 476–479, doi:10.1038/nature13032, 2014.

Fry, J. L., Kiendler-Scharr, A., Rollins, A. W., Brauers, T., Brown, S. S., Dorn, H.-P., Dubé, W. P., Fuchs, H., Mensah, A., Rohrer, F., Tillmann, R., Wahner, A., Wooldridge, P. J., and Cohen, R. C.: SOA from limonene: role of NO_3 in its generation and degradation, Atmos. Chem. Phys., 11, 3879–3894, doi:10.5194/acp-11-3879-2011, 2011.

Fuchs, H., Hofzumahaus, A., Rohrer, F., Bohn, B., Brauers, T., Dorn, H. P., Haeseler, R., Holland, F., Kaminski, M., Li, X., Lu, K., Nehr, S., Tillmann, R., Wegener, R., and Wahner, A.: Experimental evidence for efficient hydroxyl radical regeneration in isoprene oxidation, Nat. Geosci., 6, 1023–1026, doi:10.1038/ngeo1964, 2013.

Goldstein, A. H. and Galbally, I. E.: Known and unexplored organic constituents in the earth's atmosphere, Environ. Sci. Technol., 41, 1514–1521, doi:10.1021/es072476p, 2007.

Griffin, R. J., Cocker, D. R., Flagan, R. C., and Seinfeld, J. H.: Organic aerosol formation from the oxidation of biogenic hydrocarbons, J. Geophys. Res.-Atmos., 104, 3555–3567, doi:10.1029/1998jd100049, 1999.

Guenther, A., Hewitt, C. N., Erickson, D., Fall, R., Geron, C., Graedel, T., Harley, P., Klinger, L., Lerdau, M., McKay, W. A., Pierce, T., Scholes, B., Steinbrecher, R., Tallamraju, R., Taylor, J., and Zimmerman, P.: A global-model of natural volatile organic-compound emissions, J. Geophys. Res.-Atmos., 100, 8873–8892, doi:10.1029/94jd02950, 1995.

Guenther, A. B., Jiang, X., Heald, C. L., Sakulyanontvittaya, T., Duhl, T., Emmons, L. K., and Wang, X.: The Model of Emissions of Gases and Aerosols from Nature version 2.1 (MEGAN2.1): an extended and updated framework for modeling biogenic emissions, Geosci. Model Dev., 5, 1471–1492, doi:10.5194/gmd-5-1471-2012, 2012.

Hallquist, M., Wenger, J. C., Baltensperger, U., Rudich, Y., Simpson, D., Claeys, M., Dommen, J., Donahue, N. M., George, C., Goldstein, A. H., Hamilton, J. F., Herrmann, H., Hoffmann, T., Iinuma, Y., Jang, M., Jenkin, M. E., Jimenez, J. L., Kiendler-Scharr, A., Maenhaut, W., McFiggans, G., Mentel, Th. F., Monod, A., Prévôt, A. S. H., Seinfeld, J. H., Surratt, J. D., Szmigielski, R., and Wildt, J.: The formation, properties and impact of secondary organic aerosol: current and emerging issues, Atmos. Chem. Phys., 9, 5155–5236, doi:10.5194/acp-9-5155-2009, 2009.

Hao, L. Q., Yli-Pirilä, P., Tiitta, P., Romakkaniemi, S., Vaattovaara, P., Kajos, M. K., Rinne, J., Heijari, J., Kortelainen, A., Miettinen, P., Kroll, J. H., Holopainen, J. K., Smith, J. N., Joutsensaari, J., Kulmala, M., Worsnop, D. R., and Laaksonen, A.: New particle formation from the oxidation of direct emissions of pine seedlings, Atmos. Chem. Phys., 9, 8121–8137, doi:10.5194/acp-9-8121-2009, 2009.

Heald, C. L., Kroll, J. H., Jimenez, J. L., Docherty, K. S., DeCarlo, P. F., Aiken, A. C., Chen, Q., Martin, S. T., Farmer, D. K., and Artaxo, P.: A simplified description of the evolution of organic aerosol composition in the atmosphere, Geophys. Res. Lett., 37, L08803, doi:10.1029/2010gl042737, 2010.

Henry, K. M., Lohaus, T., and Donahue, N. M.: Organic aerosol yields from alpha-pinene oxidation: bridging the gap between first-generation yields and aging chemistry, Environ. Sci. Technol., 46, 12347–12354, doi:10.1021/es302060y, 2012.

Hoffmann, T., Odum, J. R., Bowman, F., Collins, D., Klockow, D., Flagan, R. C., and Seinfeld, J. H.: Formation of organic aerosols from the oxidation of biogenic hydrocarbons, J. Atoms. Chem., 26, 189–222, doi:10.1023/a:1005734301837, 1997.

Iinuma, Y., Boge, O., Miao, Y., Sierau, B., Gnauk, T., and Herrmann, H.: Laboratory studies on secondary organic aerosol formation from terpenes, Faraday Discuss., 130, 279–294, doi:10.1039/b502160j, 2005.

Jimenez, J. L., Canagaratna, M. R., Donahue, N. M., Prevot, A. S. H., Zhang, Q., Kroll, J. H., DeCarlo, P. F., Allan, J. D., Coe, H., Ng, N. L., Aiken, A. C., Docherty, K. S., Ulbrich, I. M., Grieshop, A. P., Robinson, A. L., Duplissy, J., Smith, J. D., Wilson, K. R., Lanz, V. A., Hueglin, C., Sun, Y. L., Tian, J., Laaksonen, A., Raatikainen, T., Rautiainen, J., Vaattovaara, P., Ehn, M., Kulmala, M., Tomlinson, J. M., Collins, D. R., Cubison, M. J., Dunlea, E. J., Huffman, J. A., Onasch, T. B., Alfarra, M. R., Williams, P. I., Bower, K., Kondo, Y., Schneider, J., Drewnick, F., Borrmann, S., Weimer, S., Demerjian, K., Salcedo, D., Cottrell, L., Griffin, R., Takami, A., Miyoshi, T., Hatakeyama, S., Shimono, A., Sun, J. Y., Zhang, Y. M., Dzepina, K., Kimmel, J. R., Sueper, D., Jayne, J. T., Herndon, S. C., Trimborn, A. M., Williams, L. R., Wood, E. C., Middlebrook, A. M., Kolb, C. E., Baltensperger, U., and Worsnop, D. R.: Evolution of organic aerosols in the atmosphere, Science, 326, 1525–1529, doi:10.1126/science.1180353, 2009.

Jordan, A., Haidacher, S., Hanel, G., Hartungen, E., Mark, L., Seehauser, H., Schottkowsky, R., Sulzer, P., and Mark, T. D.: A high resolution and high sensitivity proton-transfer-reaction time-of-flight mass spectrometer (PTR-TOF-MS), Int. J. Mass Spectrom., 286, 122–128, doi:10.1016/j.ijms.2009.07.005, 2009.

Kaminiski, M.: Untersuchung des photochemischen Terpenoidabbaus in der Atmosphärensimulationskammer SAPHIR, Ph.D., Universität zu Köln, Köln, 2014.

Kanakidou, M., Seinfeld, J. H., Pandis, S. N., Barnes, I., Dentener, F. J., Facchini, M. C., Van Dingenen, R., Ervens, B., Nenes, A., Nielsen, C. J., Swietlicki, E., Putaud, J. P., Balkanski, Y., Fuzzi, S., Horth, J., Moortgat, G. K., Winterhalter, R., Myhre, C. E. L., Tsigaridis, K., Vignati, E., Stephanou, E. G., and Wilson, J.: Organic aerosol and global climate modelling: a review, Atmos. Chem. Phys., 5, 1053–1123, doi:10.5194/acp-5-1053-2005, 2005.

Kiendler-Scharr, A., Wildt, J., Dal Maso, M., Hohaus, T., Kleist, E., Mentel, T. F., Tillmann, R., Uerlings, R., Schurr, U., and Wahner, A.: New particle formation in forests inhibited by isoprene emissions, Nature, 461, 381–384, doi:10.1038/nature08292, 2009a.

Kiendler-Scharr, A., Zhang, Q., Hohaus, T., Kleist, E., Mensah, A., Mentel, T. F., Spindler, C., Uerlings, R., Tillmann, R., and Wildt, J.: Aerosol mass spectrometric features of biogenic SOA: observations from a plant chamber and in rural atmospheric environments, Environ. Sci. Technol., 43, 8166–8172, doi:10.1021/es901420b, 2009b.

Kiendler-Scharr, A., Andres, S., Bachner, M., Behnke, K., Broch, S., Hofzumahaus, A., Holland, F., Kleist, E., Mentel, T. F., Rubach, F., Springer, M., Steitz, B., Tillmann, R., Wahner, A., Schnitzler, J.-P., and Wildt, J.: Isoprene in poplar emissions: effects on new particle formation and OH concentrations, Atmos. Chem. Phys., 12, 1021–1030, doi:10.5194/acp-12-1021-2012, 2012.

Kim, H., Barkey, B., and Paulson, S. E.: Real refractive indices and formation yields of secondary organic aerosol generated from photooxidation of limonene and alpha-pinene: the effect of the HC/NO_x ratio, J. Phys. Chem. A, 116, 6059–6067, doi:10.1021/jp301302z, 2012.

Kim, S., Wolfe, G. M., Mauldin, L., Cantrell, C., Guenther, A., Karl, T., Turnipseed, A., Greenberg, J., Hall, S. R., Ullmann, K., Apel, E., Hornbrook, R., Kajii, Y., Nakashima, Y., Keutsch, F. N., DiGangi, J. P., Henry, S. B., Kaser, L., Schnitzhofer, R., Graus, M., Hansel, A., Zheng, W., and Flocke, F. F.: Evaluation of HO_x sources and cycling using measurement-constrained model calculations in a 2-methyl-3-butene-2-ol (MBO) and monoterpene (MT) dominated ecosystem, Atmos. Chem. Phys., 13, 2031–2044, doi:10.5194/acp-13-2031-2013, 2013.

Kroll, J. H., Smith, J. D., Che, D. L., Kessler, S. H., Worsnop, D. R., and Wilson, K. R.: Measurement of fragmentation and functionalization pathways in the heterogeneous oxidation of oxidized organic aerosol, Phys. Chem. Chem. Phys., 11, 8005–8014, doi:10.1039/b905289e, 2009.

Lee, A., Goldstein, A. H., Keywood, M. D., Gao, S., Varutbangkul, V., Bahreini, R., Ng, N. L., Flagan, R. C., and Seinfeld, J. H.: Gas-phase products and secondary aerosol yields from the ozonolysis of ten different terpenes, J. Geophys. Res.-Atmos., 111, D07302, doi:10.1029/2005jd006437, 2006.

Lou, S., Holland, F., Rohrer, F., Lu, K., Bohn, B., Brauers, T., Chang, C.C., Fuchs, H., Häseler, R., Kita, K., Kondo, Y., Li, X., Shao, M., Zeng, L., Wahner, A., Zhang, Y., Wang, W., and Hofzumahaus, A.: Atmospheric OH reactivities in the Pearl River Delta – China in summer 2006: measurement and model results, Atmos. Chem. Phys., 10, 11243–11260, doi:10.5194/acp-10-11243-2010, 2010.

Ma, Y., Russell, A. T., and Marston, G.: Mechanisms for the formation of secondary organic aerosol components from the gas-phase ozonolysis of alpha-pinene, Phys. Chem. Chem. Phys., 10, 4294–4312, doi:10.1039/b803283a, 2008.

Mentel, Th. F., Wildt, J., Kiendler-Scharr, A., Kleist, E., Tillmann, R., Dal Maso, M., Fisseha, R., Hohaus, Th., Spahn, H., Uerlings, R., Wegener, R., Griffiths, P. T., Dinar, E., Rudich, Y., and Wahner, A.: Photochemical production of aerosols from real plant emissions, Atmos. Chem. Phys., 9, 4387–4406, doi:10.5194/acp-9-4387-2009, 2009.

Ng, N. L., Kroll, J. H., Keywood, M. D., Bahreini, R., Varutbangkul, V., Flagan, R. C., Seinfeld, J. H., Lee, A., and Goldstein, A. H.: Contribution of first- versus second-generation products to secondary organic aerosols formed in the oxidation of biogenic hydrocarbons, Environ. Sci. Technol., 40, 2283–2297, doi:10.1021/es052269u, 2006.

Ng, N. L., Chhabra, P. S., Chan, A. W. H., Surratt, J. D., Kroll, J. H., Kwan, A. J., McCabe, D. C., Wennberg, P. O., Sorooshian, A., Murphy, S. M., Dalleska, N. F., Flagan, R. C., and Seinfeld, J. H.: Effect of NO_x level on secondary organic aerosol (SOA) formation from the photooxidation of terpenes, Atmos. Chem. Phys., 7, 5159–5174, doi:10.5194/acp-7-5159-2007, 2007.

Ng, N. L., Canagaratna, M. R., Zhang, Q., Jimenez, J. L., Tian, J., Ulbrich, I. M., Kroll, J. H., Docherty, K. S., Chhabra, P. S., Bahreini, R., Murphy, S. M., Seinfeld, J. H., Hildebrandt, L., Donahue, N. M., DeCarlo, P. F., Lanz, V. A., Prévôt, A. S. H., Dinar, E., Rudich, Y., and Worsnop, D. R.: Organic aerosol components observed in Northern Hemispheric datasets from Aerosol Mass Spectrometry, Atmos. Chem. Phys., 10, 4625–4641, doi:10.5194/acp-10-4625-2010, 2010.

Ng, N. L., Canagaratna, M. R., Jimenez, J. L., Chhabra, P. S., Seinfeld, J. H., and Worsnop, D. R.: Changes in organic aerosol composition with aging inferred from aerosol mass spectra, Atmos. Chem. Phys., 11, 6465–6474, doi:10.5194/acp-11-6465-2011, 2011.

Ortega, I. K., Suni, T., Boy, M., Grönholm, T., Manninen, H. E., Nieminen, T., Ehn, M., Junninen, H., Hakola, H., Hellén, H., Valmari, T., Arvela, H., Zegelin, S., Hughes, D., Kitchen, M., Cleugh, H., Worsnop, D. R., Kulmala, M., and Kerminen, V.-M.: New insights into nocturnal nucleation, Atmos. Chem. Phys., 12, 4297–4312, doi:10.5194/acp-12-4297-2012, 2012.

Pathak, R., Donahue, N. M., and Pandis, S. N.: Ozonolysis of beta-pinene: temperature dependence of secondary organic aerosol mass fraction, Environ. Sci. Technol., 42, 5081–5086, doi:10.1021/es070721z, 2008.

Pathak, R. K., Stanier, C. O., Donahue, N. M., and Pandis, S. N.: Ozonolysis of alpha-pinene at atmospherically relevant concentrations: temperature dependence of aerosol mass fractions (yields), J. Geophys. Res.-Atmos., 112, D03201, doi:10.1029/2006jd007436, 2007.

Pfaffenberger, L., Barmet, P., Slowik, J. G., Praplan, A. P., Dommen, J., Prévôt, A. S. H., and Baltensperger, U.: The link between organic aerosol mass loading and degree of oxygenation: an α-pinene photooxidation study, Atmos. Chem. Phys., 13, 6493–6506, doi:10.5194/acp-13-6493-2013, 2013.

Presto, A. A., Hartz, K. E. H., and Donahue, N. M.: Secondary organic aerosol production from terpene ozonolysis. 2. Effect of NO_x concentration, Environ. Sci. Technol., 39, 7046–7054, doi:10.1021/es050400s, 2005.

Presto, A. A. and Donahue, N. M.: Investigation of alpha-pinene plus ozone secondary organic aerosol formation at low total aerosol mass, Environ. Sci. Technol., 40, 3536–3543, doi:10.1021/es052203z, 2006.

Rohrer, F., Bohn, B., Brauers, T., Brüning, D., Johnen, F.-J., Wahner, A., and Kleffmann, J.: Characterisation of the photolytic HONO-source in the atmosphere simulation chamber SAPHIR, Atmos. Chem. Phys., 5, 2189–2201, doi:10.5194/acp-5-2189-2005, 2005.

Saathoff, H., Naumann, K.-H., Möhler, O., Jonsson, Å. M., Hallquist, M., Kiendler-Scharr, A., Mentel, Th. F., Tillmann, R., and Schurath, U.: Temperature dependence of yields of secondary organic aerosols from the ozonolysis of α-pinene and limonene, Atmos. Chem. Phys., 9, 1551–1577, doi:10.5194/acp-9-1551-2009, 2009.

Salo, K., Hallquist, M., Jonsson, Å. M., Saathoff, H., Naumann, K.-H., Spindler, C., Tillmann, R., Fuchs, H., Bohn, B., Rubach, F., Mentel, Th. F., Müller, L., Reinnig, M., Hoffmann, T., and

Donahue, N. M.: Volatility of secondary organic aerosol during OH radical induced ageing, Atmos. Chem. Phys., 11, 11055–11067, doi:10.5194/acp-11-11055-2011, 2011.

Shilling, J. E., Chen, Q., King, S. M., Rosenoern, T., Kroll, J. H., Worsnop, D. R., McKinney, K. A., and Martin, S. T.: Particle mass yield in secondary organic aerosol formed by the dark ozonolysis of α-pinene, Atmos. Chem. Phys., 8, 2073–2088, doi:10.5194/acp-8-2073-2008, 2008.

Shilling, J. E., Chen, Q., King, S. M., Rosenoern, T., Kroll, J. H., Worsnop, D. R., DeCarlo, P. F., Aiken, A. C., Sueper, D., Jimenez, J. L., and Martin, S. T.: Loading-dependent elemental composition of α-pinene SOA particles, Atmos. Chem. Phys., 9, 771–782, doi:10.5194/acp-9-771-2009, 2009.

Spracklen, D. V., Jimenez, J. L., Carslaw, K. S., Worsnop, D. R., Evans, M. J., Mann, G. W., Zhang, Q., Canagaratna, M. R., Allan, J., Coe, H., McFiggans, G., Rap, A., and Forster, P.: Aerosol mass spectrometer constraint on the global secondary organic aerosol budget, Atmos. Chem. Phys., 11, 12109–12136, doi:10.5194/acp-11-12109-2011, 2011.

Tillmann, R., Hallquist, M., Jonsson, Å. M., Kiendler-Scharr, A., Saathoff, H., Iinuma, Y., and Mentel, Th. F.: Influence of relative humidity and temperature on the production of pinonaldehyde and OH radicals from the ozonolysis of α-pinene, Atmos. Chem. Phys., 10, 7057–7072, doi:10.5194/acp-10-7057-2010, 2010.

Whalley, L. K., Edwards, P. M., Furneaux, K. L., Goddard, A., Ingham, T., Evans, M. J., Stone, D., Hopkins, J. R., Jones, C. E., Karunaharan, A., Lee, J. D., Lewis, A. C., Monks, P. S., Moller, S. J., and Heard, D. E.: Quantifying the magnitude of a missing hydroxyl radical source in a tropical rainforest, Atmos. Chem. Phys., 11, 7223–7233, doi:10.5194/acp-11-7223-2011, 2011.

Yu, J. Z., Cocker, D. R., Griffin, R. J., Flagan, R. C., and Seinfeld, J. H.: Gas-phase ozone oxidation of monoterpenes: Gaseous and particulate products, J. Atoms. Chem., 34, 207–258, doi:10.1023/a:1006254930583, 1999.

Zhang, J. Y., Hartz, K. E. H., Pandis, S. N., and Donahue, N. M.: Secondary organic aerosol formation from limonene ozonolysis: Homogeneous and heterogeneous influences as a function of NO_x, J. Phys. Chem. A, 110, 11053–11063, doi:10.1021/jp062836f, 2006.

Zhang, Q., Jimenez, J. L., Canagaratna, M. R., Ulbrich, I. M., Ng, N. L., Worsnop, D. R., and Sun, Y. L.: Understanding atmospheric organic aerosols via factor analysis of aerosol mass spectrometry: a review, Anal. Bioanal. Chem., 401, 3045–3067, doi:10.1007/s00216-011-5355-y, 2011.

Title Page
Abstract | Introduction
Conclusions | References
Tables | Figures
◀I | ▶I
◀ | ▶
Back | Close
Full Screen / Esc
Printer-friendly Version
Interactive Discussion

Ziemann, P. J. and Atkinson, R.: Kinetics, products, and mechanisms of secondary organic aerosol formation, Chem. Soc. Rev., 41, 6582–6605, doi:10.1039/c2cs35122f, 2012.

Table 1. Summary of experimental conditions. All experiments were performed at initial RH 75 % and NO_x <1 ppb.

Experiment type	VOC type	VOC initial (ppb)	[OH] (10^6 molecules cm^{-3})	Initial O_3 (ppb)	Average T (K)	Initial mass ($\mu g\, m^{-3}$)	Rate coefficient ($molecule^{-1}\, cm^3\, s^{-1}$)[b]
OH oxidation	α-pinene	4	6.4	1.0	299	6.1×10^{-3}	5.25×10^{-11}
	β-pinene	4	6.2	2.5	301	9.5×10^{-3}	7.89×10^{-11}
	limonene	4	6.4	2.2	298	12.2×10^{-3}	1.64×10^{-11}
Ozonolysis	α-pinene	4	NDs[a]	136	289	9.2×10^{-3}	8.72×10^{-16}
	β-pinene	4	NDs	760	294	5.7×10^{-3}	1.50×10^{-16}
	limonene	4	NDs	136	290	11.7×10^{-3}	2.08×10^{-16}

[a] Below the detection limit of instruments (0.3×10^6 molecules cm^{-3}).

[b] Atkinson and Arey (2003).

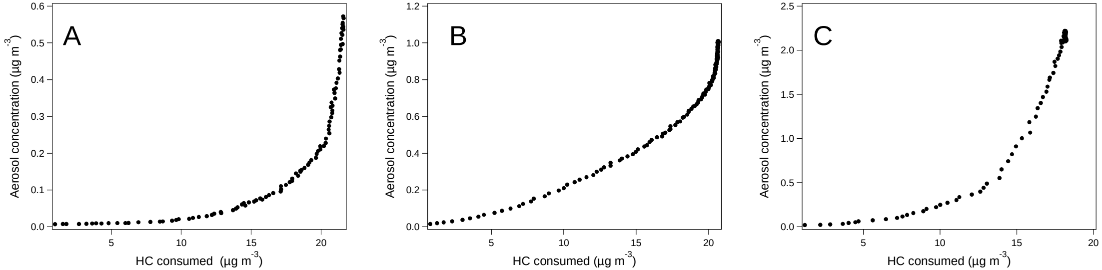

Fig. 1. Time dependent growth curve of aerosol from the OH oxidation of α-pinene **(a)**, β-pinene **(b)** and limonene **(c)** as function of hydrocarbon(HC) consumed (monoterpene here).

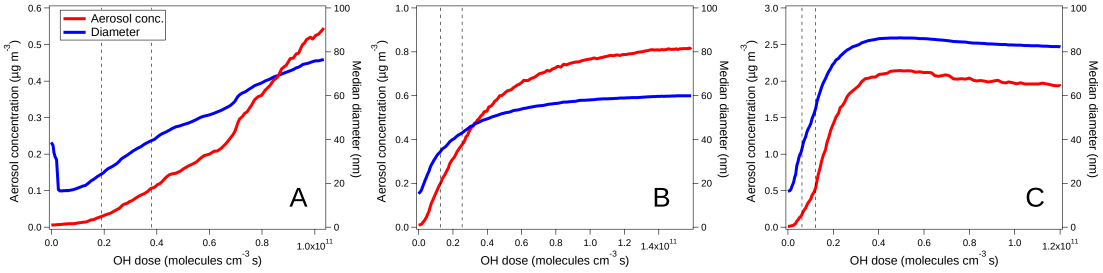

Fig. 2. Particle mass concentration and median diameter as a function of OH dose for the OH oxidation of α-pinene **(a)**, β-pinene **(b)** and limonene **(c)**. The dashed vertical lines correspond to the one and two lifetimes each monoterpene in respect to OH oxidation. The lifetime is the time when the monoterpene concentration decreases to 1/e of the initial concentration.

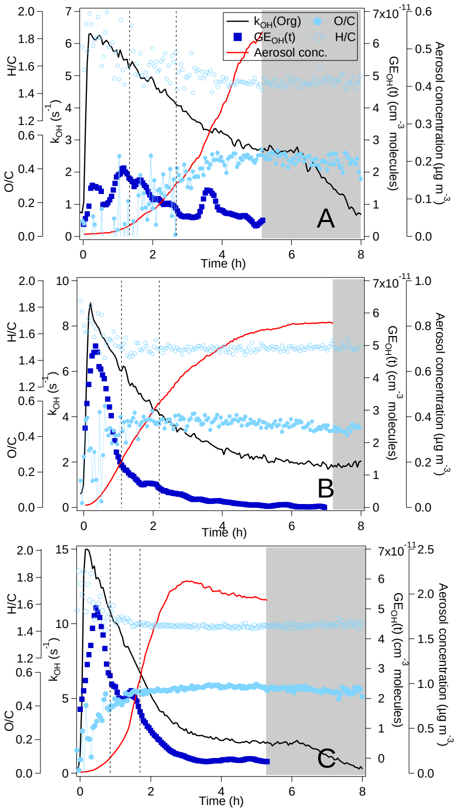

Fig. 3. Time series of $GE_{OH}(t)$ (particle mass growth efficiency in respect to the reaction of OH with organics, refer to the text for details. For clarity 7 points moving average is shown.), k_{OH} (OH reactivity) of organics, O/C and H/C from AMS data, and aerosol mass concentration in the OH oxidation of α-pinene **(a)**, β-pinene **(b)** and limonene **(c)**. The shaded area shows the dark period. The dashed vertical lines in each panel show the one and two lifetimes of the monoterpene.

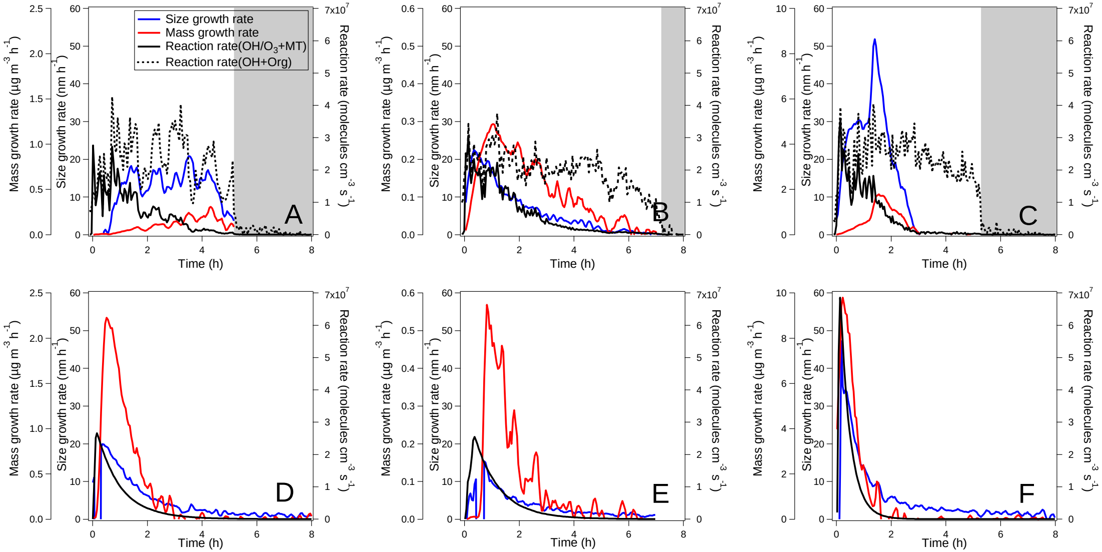

Fig. 4. Particle size growth rate, mass growth rate and reaction rate of OH or O_3 with α-pinene **(a, d)**, β-pinene **(b, e)** and limonene **(c, f)**. The top panels are from OH oxidation (the shaded area shows the dark period) and bottom panels from ozonolysis in the presence of CO as OH scavenger. For the OH oxidation, the total reaction rate of OH with all organics is also shown.

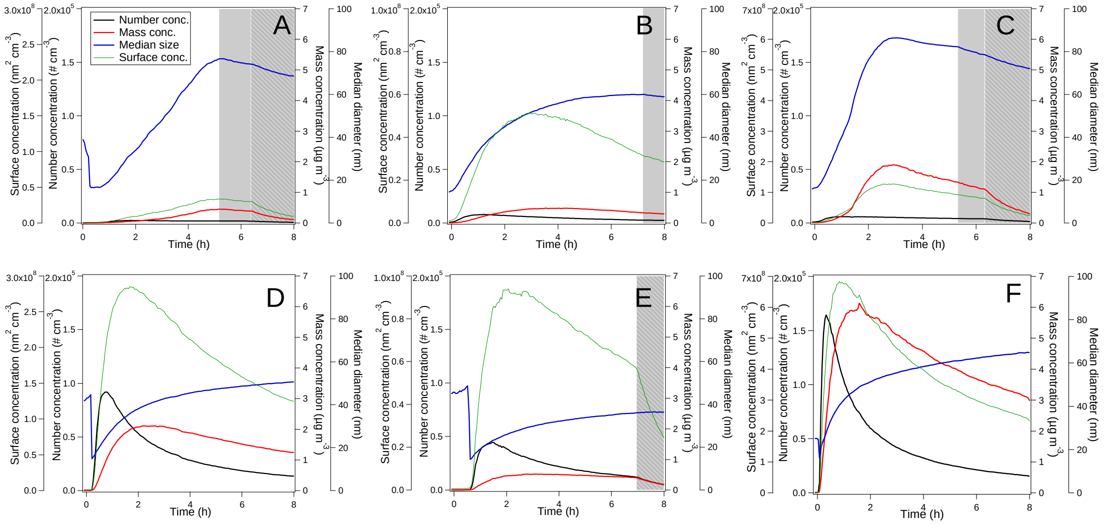

Fig. 5. Particle number concentration, mass concentration (not corrected for losses), surface concentration and median diameter of the aerosol from *α*-pinene **(a, d)**, *β*-pinene **(b, e)** and limonene **(c, f)**. The top panels are from OH oxidation (the gray shaded area shows the dark period) and bottom panels from ozonolysis. The grey hatched area corresponds to the flushing out period.

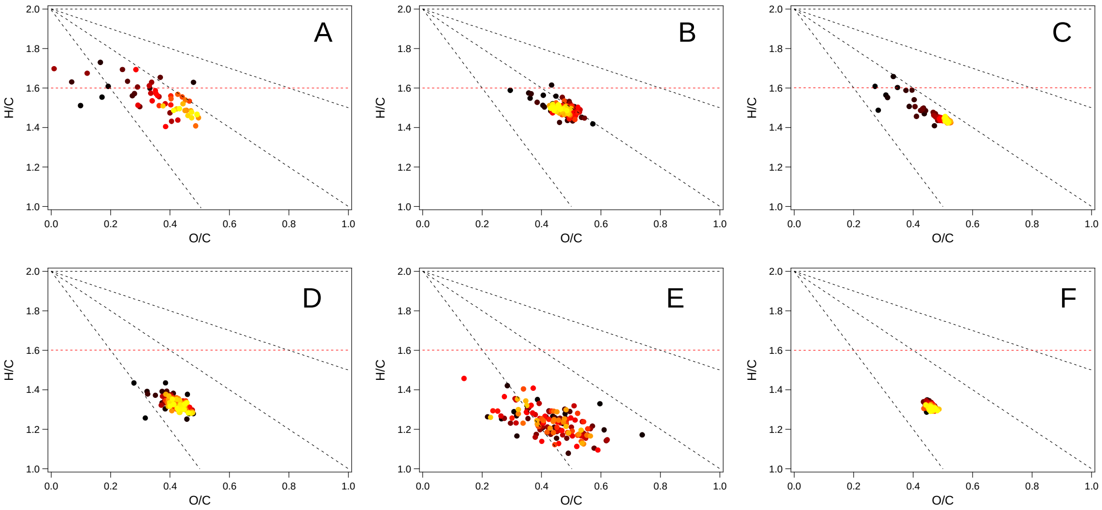

Fig. 6. H/C and O/C ratio of SOA from the OH oxidation and ozonolysis of α-pinene **(a, d)**, β-pinene **(b, e)** and limonene **(c, f)**. The top panels are from OH oxidation and bottom panels from ozonolysis. Dark color denotes the beginning of the experiments and yellow denotes the later period. The red dashed line correspond to H/C = 1.6. The black dashed lines correspond to the slope of −2, −1 and −0.5.

Title Page
Abstract
Introduction
Conclusions
References
Tables
Figures
◀◀
▶▶
◀
▶
Back
Close
Full Screen / Esc
Printer-friendly Version
Interactive Discussion

Title Page
Abstract Introduction
Conclusions References
Tables Figures
◀I ▶I
◀ ▶
Back Close
Full Screen / Esc
Printer-friendly Version
Interactive Discussion

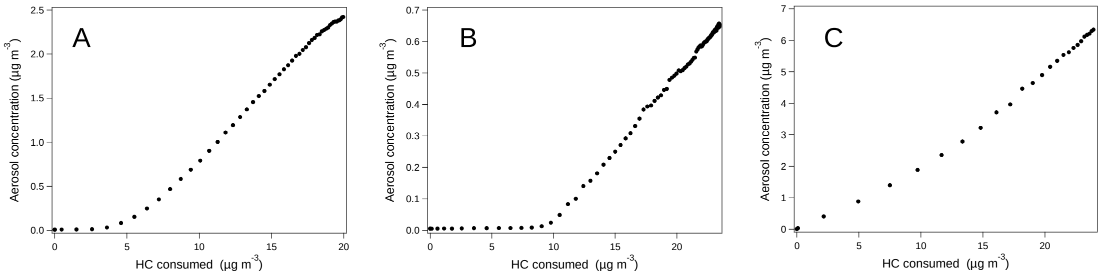

Fig. A1. Time dependent growth curve of the aerosol from ozonolysis of α-pinene **(a)**, β-pinene **(b)** and limonene **(c)**.

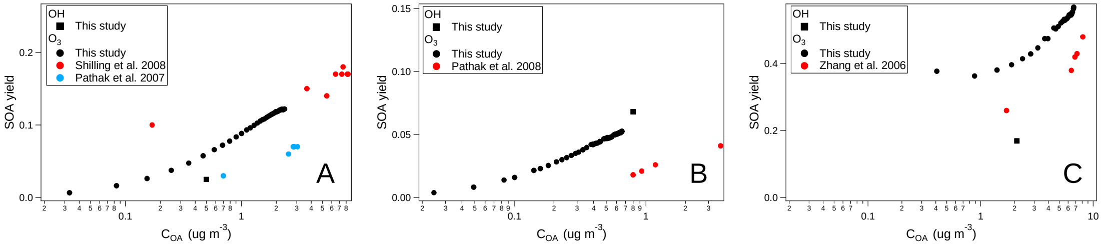

Fig. A2. Aerosol yield from the OH oxidation and ozonolysis of of α-pinene **(a)**, β-pinene **(b)** and limonene **(c)** as a function of organic aerosol loading (C_{OA}). Data from literature at the similar organic mass loading with this study are shown. Experimental conditions including the OH scavenger, temperature and RH etc. are not exactly the same as these studies in the literature.